Effect of different refining slag systems on the cleanliness of molten steel for carbon structural steel

by S. Zhao*, L. Ma*, Y. Tao*, S.P. He†, and M.Y. Zhu‡

Synopsis

The effect of two refining slags (A: 1.0–1.8 CaO/Al$_2$O$_3$ ratio, 11–20 wt% SiO$_2$; and B: 1.0–1.2 CaO/SiO$_2$ ratio, 25–35 wt% Al$_2$O$_3$) on the inclusion morphology of a carbon structural steel (Q235B) was studied by controlling the balance between the steel and the refining slag at 1600°C in a Si–Mo resistance laboratory furnace. The results showed that most of the inclusions in the molten steel balanced with slag A were formed by a low-melting CaO–MgO–Al$_2$O$_3$–SiO$_2$ system with a total oxygen content (T[O]) being fixed at 6–13 ppm. The inclusions in liquid steel balanced with the slag B were mostly formed by the CaO–MnO–Al$_2$O$_3$–SiO$_2$ system, with T[O] controlled to 19–26 ppm. The overall size of the inclusions under balance conditions was higher in the steel reacted with the slag B than that reacted with slag A, with the latter showing more inclusions smaller than 3 μm. In order to generate a large number of spherical CaO–MgO–Al$_2$O$_3$–SiO$_2$ inclusions smaller than 3 μm while decreasing the T[O] in the resulting steel, the composition of slag A should be used. This composition allowed improving the cleanliness of the slab, and is also advantageous for the castability of the molten steel.

Keywords
carbon structural steel, cleanliness, refining slag, inclusions.

Introduction

The sample used in this study was a typical carbon steel manufactured by CQ Steel. The galvanized, tinned, and plastic composite steel plates made of the original plates are used extensively for decorative panels, general dust pipes, drums, instrument cases, switchboxes, and train cars, among other uses. The target control composition is shown in Table I. The S and P contents are usually fixed during production below 0.020 and 0.025 wt%, respectively, with the aim of reducing longitudinal cracks on the slab surface.

This type of carbon steel (Q235B) is manufactured by numerous steel companies worldwide owing to the high market demand and simple production process. The main production issues are related to the control of the castability of the molten steel while reducing costs. The production route for Q235B followed by CQ Steel is currently as follows: converter smelting → composition adjustment by sealed argon bubbling (CAS) → continuous casting. Although this route ensures smooth production, ladle furnace (LF) and Ca treatments are usually employed to

solve occasional issues. In order to ensure a high sulphur capacity, the refining slag compositions should have a CaO/SiO$_2$ ratio of 3–4, a SiO$_2$ content fixed at 17 wt%, and an Al$_2$O$_3$ content of approximately 20 wt% (the area delimited by circles in Figure 1). This results in a slag melting temperature of approximately 1700°C. In this case, the following issues appear: (i) the content of the high-melting-point Al$_2$O$_3$ inclusions is higher and the castability of the molten steel is unstable; (ii) the clogging ratio of the nozzle is close to 20% in the all production heats, thereby resulting in the molten steel not satisfying the casting process; and (iii) the presence of longitudinal cracks on the slab surface, typically caused by the above reasons, leading to slab offline inspection and cleaning and the product not meeting the cast-rolling compact layout and hot charging requirements.

The LF refining process was employed in other companies in the past (Peng *et al.*, 2007; Xu *et al.*, 2009; Zhi *et al.*, 2004; Li, He, and Zhang, 2010). However, the CQ Steel plant used CAS processing, and more stringent requirements at the operating level have been proposed. With this background, this investigation was aimed at achieving high efficiency and low-cost production by adjusting the refining slagging process to ensure cleanliness of the steel.

Selection of the refining slag

To overcome these issues, a low-melting-point slag can be used to avoid the solid phase generated from the steel–slag reaction. Since slag washing is carried out during tapping

* *College of Materials Science and Engineering, Hebei University of Engineering, Handan, China.*
† *College of Materials Science and Engineering, Chongqing University, Chongqing, China.*
‡ *College of Metallurgy Engineering, Northeastern University, Shenyang, China.*

Effect of different refining slag systems on the cleanliness of molten steel

Table I

Target control compositions, wt%

	C	Si	Mn	P	S	Cr	Cu	As
Control requirements Target	0.12–0.19 0.16	≤0.30 0.20	0.20–0.40 0.30	≤0.045 ≤0.030	≤0.045 ≤0.025	≤0.30 ≤0.30	≤0.30 ≤0.30	≤0.08 ≤0.08
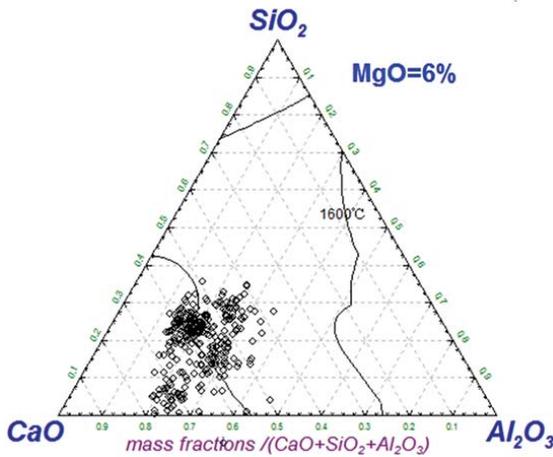
Figure 1—Composition of the original refining slag

under dynamic conditions, complete contact between the slag and the steel is ensured, thereby allowing inclusions to be immediately assimilated and absorbed by the refining slag at the beginning of the refining process and resulting in smooth casting and enhanced product performance. The appropriate refining slag should be selected by the following criteria:

(1) The slag should have an appropriate melting point and viscosity such that fluidity is maintained
(2) The oxidizability of the slag should be low so that it does not easily react with the Al in the steel. Thus, the formation of Al_2O_3 inclusions is avoided
(3) The slag should have a good desulphurization ability
(4) The inclusions in the steel should be assimilated to the low-melting-point area for them to be easily absorbed by the slag.

In addition, when a strong deoxidizing treatment (deoxidation mainly by Fe–Al) is used during steel tapping, the slag composition should be selected in combination with the actual situation of the steel, and the following conditions must be met:

(1) In agreement with calculated results, the proportion of Si deoxidation products should account for no less than 11% of the final slag weight to ensure a basicity of the top slag higher than 2.0 while suppressing the slag–steel reaction (i.e., $a_{(Al_2O_3)}^{0.5}/a_{(SiO_2)}^{0.75} > 63.5$), and the SiO_2 content must be fixed below 20%.

$$[Al]+0.75(SiO_2)=0.5(Al_2O_3)+0.75[Si]$$

$$\Delta G^o = -658300 + 107.2T \quad J/mol \tag{1}$$

$$\Delta G = \Delta G^o + RT \ln \frac{(a_{Al_2O_3})^2(a_{Si})^3}{(a_{SiO_2})^3(a_{Al})^4} \tag{2}$$

(2) The MgO content should be 6–9% in order to reduce lining erosion and the melting point of the slag
(3) Yoon, Heo, and Kim (2002) pointed out that rate of deoxidation improves when the slag contains $CaO/Al_2O_3 \geq 1.0$. According to thermodynamic calculated results, the MgO content is restricted to 8% when the CaO/Al_2O_3 ratio is in the range of 1.2–1.8. Under these conditions, the slag should present good fluidity and a melting point below 1500°C
(4) The refining slag inevitably carries CaF_2 with the impurities. Thus, it contains a certain amount of F^- and, from an environmental point of view, this content should not exceed 3 wt%.

According to the thermodynamic calculations controlling oxide inclusions, for the melting point of the inclusions to be lower than 1500°C in the $CaO–SiO_2–Al_2O_3–6\%MgO$ system, the chemical composition should be as listed in Table II (corresponding to area A in Figure 3).

When a weak deoxidizing treatment is used during the tapping process (deoxidation mainly by Fe–Si, with little or no use of Fe–Al), the reaction products are SiO_2, Al_2O_3, and minor amounts of MnO. In this case, the assimilation ability of the slag for SiO_2 and Al_2O_3 during the design time should
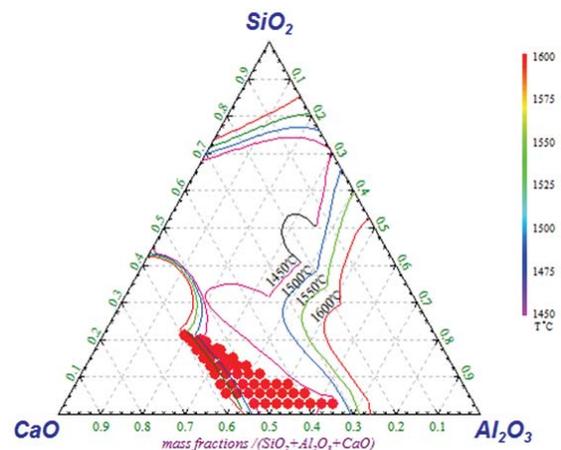

Figure 2—Range of refining slag compositions for inhibiting reaction [1] in the CaO–SiO_2–Al_2O_3–6%MgO system (red circles)

Table II

Chemical composition and physical properties of the refining slag (wt%)

CaO	Al_2O_3	SiO_2	MgO	F-	Melting point
40–52	30–38	11–20	6–9	≤3	≤ 1500°C

Effect of different refining slag systems on the cleanliness of molten steel
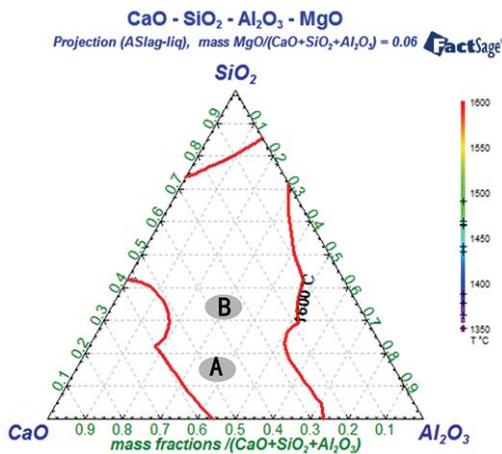

Figure 3—Composition control of the slag

be such that low-melting-point inclusions with improved buoyancy are formed while reducing the amount of precipitates during the casting process. In the refining process, to improve the floating of the low-melting inclusions and their rate of removal, high argon flows and stirring times should be ensured. According to thermodynamic calculations, to ensure that the $MnO–SiO_2–Al_2O_3$ inclusions are in the liquid state, the oxygen content of the liquid steel should be no higher than 25 ppm under balance conditions, and the composition of the slag should be in the range: $w(CaO) = 34–38\%$, $w(SiO_2) = 32–36\%$, $w(Al_2O_3) = 25–35\%$, and $w(MgO) = 6\%$ (area B in Figure 3).

The main purpose of this laboratory study was to analyse and study the relationship between the slag components, the molten steel, and the inclusions in the steel when the composition of the slag (areas A or B in the $CaO–SiO_2–Al_2O_3–6\%MgO$ system: Figure 3) is balanced with the liquid carbon steel under different deoxidation conditions. This study would provide a new solution to improve the castability of carbon structural steel while enhancing the cleanliness of the steel product.

Experimental process

Materials

The experimental steel was a Q235B steel produced by CQ Steel mill with dimensions 27 mm × 27 mm × 60 mm. Each sample was analysed to determine the exact composition. The basic chemical composition of the experimental steel is shown in Table III.

The compositions of slags used in the experiments are shown in Tables IV and V. The first slag (slag A, Figure 3) used the $CaO–Al_2O_3$ system, with a CaO/Al_2O_3 ratio of 1.0–1.8 and a SiO_2 content of 11–20 wt%. The second slag (slag B, Figure 3) used the $CaO–Al_2O_3$ system with a CaO/SiO_2 ratio of 1.0–1.2 and an Al_2O_3 content in the range 25–35 wt%. The MgO, SiO_2, and Al_2O_3 contents in the slag were adjusted with analytically pure oxides; to prevent moisture absorption, CaO was replaced by $CaCO_3$. All the oxides were pulverized and pre-dehydrated.

Equipment and experimental procedure

A high-temperature Si–Mo furnace was selected for the steel-

slag equilibrium experiments. The furnace and accessory laboratory equipment is shown in Figure 4.

Table III

Basic composition of the experimental steel, wt%

C	Si	Mn	P	S	Alt	Als
0.14	0.19	0.35	0.017	0.006	0.005	0.003

Table IV

Experimental plan for slag A

Sample	Percentage of slag A components, wt%						
	CaO/Al$_2$O$_3$	CaO	SiO$_2$	Al$_2$O$_3$	MgO	CaF$_2$	Melting point,°C
A1	1.0	39	11	39	6	5	1470
A2	1.2	42.55	11	35.45	6	5	1410
A3	1.4	45.5	11	32.5	6	5	1476
A4	1.6	48	11	30.0	6	5	1538
A5	1.8	50.14	11	27.86	6	5	1584
A6	1.0	36	17	36	6	5	1540
A7	1.2	39.27	17	32.73	6	5	1503
A8	1.4	42	17	30.0	6	5	1468
A9	1.6	44.31	17	27.69	6	5	1430
A10	1.8	46.29	17	25.71	6	5	1454
A11	1.2	40.91	14	34.09	6	5	1464
A12	1.2	37.64	20	31.36	6	5	1521
A13	1.4	43.75	14	31.25	6	5	1420
A14	1.4	40.25	20	28.75	6	5	1495
A15	1.6	46.15	14	28.85	6	5	1476
A16	1.6	42.46	20	26.54	6	5	1471

Table V

Experimental plan for slag B

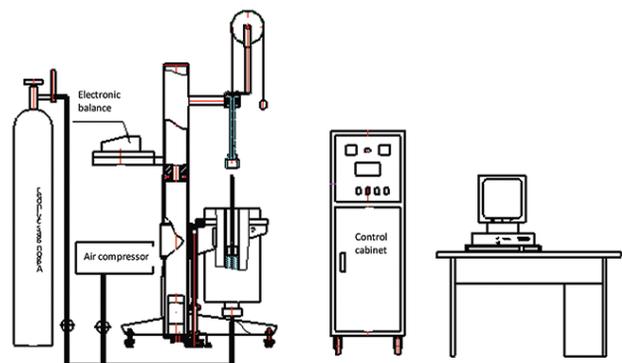| Sample	Percentage of slag B components, wt%					
	CaO/SiO$_2$	CaO	SiO$_2$	Al$_2$O$_3$	MgO	Melting point, °C
B1	1.0	32	32	30	6	1447
B2	1.2	34.91	29.09	30	6	1485
B3	1.0	34.50	34.50	25	6	1400
B4	1.2	37.64	31.36	25	6	1471
B5	1.0	29.5	29.5	35	6	1503
B6	1.2	32.18	26.82	35	6	1499

Figure 4—Sketch of the laboratory apparatus

Effect of different refining slag systems on the cleanliness of molten steel

The entire experiment process was carried out under 99.9% argon (argon flow: 2 L/min, furnace temperature 1600 ± 1°C). The temperature was measured by a double (platinum and rhodium) thermocouple, and the data was displayed on the instrument–computer interface. In order to avoid steel breakout, a MgO crucible (inner diameter φ = 44 mm, inner height H = 66 mm) was placed in a graphite-lined crucible. The average weight of the steel sample was 400 g in the MgO crucible (slag accounted for 30%). The crucible containing the steel sample was preheated to the specified temperature in the resistance furnace and subsequently placed in the thermostat zone of the furnace. Once the thermocouple temperature reached 1600°C, this temperature was maintained for 60 minutes (determined by the pre-equilibrium reaction time), after which the crucible was quickly removed and cooled in water. Finally, the steel and the slag were separately removed from the cracked crucibles. The elemental composition of the samples was determined by X-ray fluorescence (XRF) using an XRF-1800 device. Subsequently, the steel was cut in the middle for metallographic studies using scanning electron microscopy (SEM). The sizes, shapes, and compositions of the inclusions were analysed by an Axiovert 200 MAT metallurgical microscope and a TESCAN VEGA III scanning electron microscope.

According to the requirements of the experiment, different CaO–Al$_2$O$_3$–SiO$_2$ slag samples were prepared

To investigate the effect of the components of slag A on the steel inclusions, both the CaO/Al$_2$O$_3$ ratio (1.0, 1.2, 1.4, 1.6, and 1.8) and the SiO$_2$ content (11, 14, 17, and 20 wt%) were varied while maintaining the steel composition constant. At the same time, a set of blank tests was prepared.

In order to study the effect of the components of slag B on the steel inclusions, both the CaO/SiO$_2$ ratio (1.0 and 1.2) and the Al$_2$O$_3$ content (25, 30, and 35 wt%) were varied while maintaining the steel composition constant.

Analysis and discussion

Experimental results

The components of the slag have a very important influence on the steel composition and the types of inclusions. Thus, when a dynamic balance is reached between the slag and the steel, the elements in the steel simultaneously reach equilibrium with the inclusions. Thus, both the inclusions and the steel composition can be controlled by the slag. According to Equations [3]–[6], the slag basicity and the Al$_2$O$_3$, FeO, and MnO contents in the slag have a very close relationship with the elements and inclusions in the steel (Ohta and Suito, 1996a; Richard and Chipman, 1965; Huang, 2008).

$$4[Al]_{steel} + 3(SiO_2)_{slag} = 2(Al_2O_3)_{slag} + 3[Si]_{steel} \qquad [3]$$

$$2[Al]_{steel} + 3(FeO)_{slag} = (Al_2O_3)_{slag} + 3[Fe]_{steel} \qquad [4]$$

$$2[Al]_{steel} + 3(MnO)_{slag} = (Al_2O_3)_{slag} + 3[Mn]_{steel} \qquad [5]$$

$$(Al_2O_3)_{slag} = (Al_2O_3)_{inclusion} \qquad [6]$$

The components of slags A and B are shown in Tables IV and V, respectively. Slag A had a basicity range of 2.5–3.5 and an average Al$_2$O$_3$ content of approximately 32 wt%. Slag B had a CaO/Al$_2$O$_3$ ratio of 0.8–1.5 and an average SiO$_2$ content of approximately 31 wt%. The T[O] content and the types of inclusions were controlled by the different slag systems, and the experiments were carried out on the same equipment and under the same conditions to avoid any effect of extraneous conditions. The T[O] and [N] contents in the samples were measured on an ELTRA ON-900 analyser, and the analysis results (gas content and slag components) after reaction are listed in Table VI.

Control of the slag components with different slag systems under equilibrium conditions

The compositions of slags A and slag B after reaching chemical equilibrium with the carbon steel (1 hour) are shown in Figures 5 and 6. As shown, the CaO/Al$_2$O$_3$ ratio of slag A ranged from 1.51 to 2.50 under equilibrium conditions, and this ratio was reduced to 1.31–1.89 for slag B. The SiO$_2$ contents were 11.2–20.4 and 27.60–30.44 wt% for slags A and B, respectively, and the (FeO + MnO) contents were 0.31–1.54 and 0.48–1.22 wt% respectively. Compared with slag B, slag A had higher CaO/Al$_2$O$_3$ ratios, lower SiO$_2$ contents, and lower oxidizability in agreement with the higher CaO/Al$_2$O$_3$ ratios in the slag.

When the reaction of the slag and liquid carbon steel was balanced, the sulphur contents in the slag were 0.044–0.065 and 0.019–0.029 wt% for slags A and B, respectively. As can be seen from the relationship between the slag composition and its sulphur content (Figures 7 and 8), the average sulphur content was 0.023 wt% in slag B, while the average

---

Table VI

Analysis of the gas content in the steel and the slag components

Sample	Slag components, wt%				Gas content, ppm	
	(CaO+MgO)/ SiO$_2$	CaO/ Al$_2$O$_3$	FeO+ MnO	(S)	T[O]	[N]
A1	4.79	1.55	0.65	0.065	8	48
A2	5.01	1.73	0.33	0.059	8	68
A3	5.15	1.97	0.35	0.059	10	42
A4	4.82	2.14	0.70	0.050	8	45
A5	5.95	2.41	0.31	0.057	8	57
A6	2.84	1.51	0.44	0.044	13	62
A7	3.41	1.95	0.39	0.048	12	40
A8	3.28	2.02	0.39	0.051	10	47
A9	3.38	2.29	0.34	0.048	9	56
A10	2.79	2.15	1.54	0.062	10	54
A11	3.89	1.72	0.44	0.057	6	27
A12	2.75	1.78	0.37	0.054	11	53
A13	4.09	1.96	0.51	0.051	9	42
A14	3.02	2.33	0.43	0.054	12	33
A15	3.47	2.44	0.42	0.052	11	43
A16	4.43	2.50	0.43	0.063	8	39
B1	1.72	1.89	0.88	0.022	22	47
B2	1.57	1.63	1.22	0.029	22	37
B3	1.46	1.32	0.73	0.019	26	28
B4	1.61	1.88	0.70	0.023	20	51
B5	1.53	1.59	0.90	0.025	19	41
B6	1.58	1.31	0.48	0.019	24	37
Blank sample					28	97

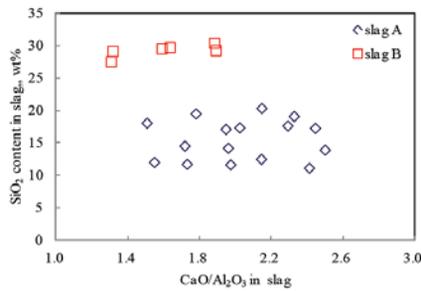# Effect of different refining slag systems on the cleanliness of molten steel

Figure 5—SiO$_2$ content as a function of the CaO/Al$_2$O$_3$ ratio in the slag
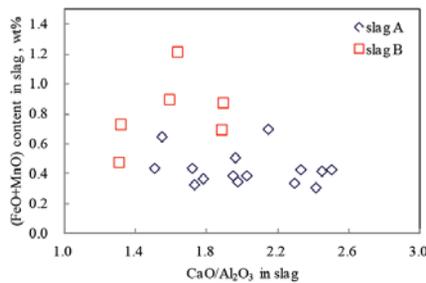

Figure 6—(FeO + MnO) content as a function of the CaO/Al$_2$O3$_2$ ratio in the slag

sulphur content of slag A was 0.055 wt%, an increase of 139%. Thus, slag A showed a stronger desulphurization capacity (higher sulphur capacity) than slag B.

The desulphurization reaction between the slag and the steel can be expressed by the following molecular or ionic theory (Ohta and Suito, 1996b). According to metallurgical principles and Equations [7] and [10], the slag must: (i) first increase its CaO content to reduce the sulphur content in liquid steel, and (ii) reduce the oxygen potential in the steel. Since slag A had a higher CaO/Al$_2$O$_3$ ratios and integrated basicity ((CaO + MgO)/SiO$_2$ ratio) compared to slag B, the former showed a higher desulphurization capacity.

Molecular theory $(CaO) + [S] = (CaS) + [O]$
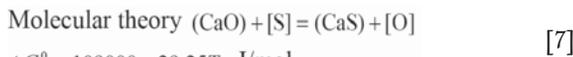
$$\Delta G^0 = 109000 - 29.25T \quad J/mol \qquad [7]$$

Equilibrium constant $\lg K_1 =$

$$\lg \frac{a_{CaS} \cdot a_{[O]}}{a_{CaO} \cdot a_{[S]}} = \frac{-5693}{T} + 1.528 \qquad [8]$$

Ionic theory $(O^{2-}) + [S] = (S^{2-}) + [O]$
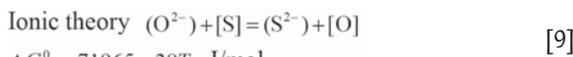
$$\Delta G^0 = 71965 - 38T \quad J/mol \qquad [9]$$

Equilibrium constant $\lg K_2 =$

$$\lg \frac{a_{S^{2-}} \cdot a_{[O]}}{a_{[S]} \cdot a_{O^{2-}}} = -\frac{6500}{T} + 2.625 \qquad [10]$$

Control of the T[O] content in steel with different slag systems under equilibrium conditions

The T[O] content in the carbon steel balanced with slag A was in the range of 6–13 ppm, and 19–26 ppm for slag B. The average oxygen content was thus 15 ppm higher in the steel balanced with slag B, but the T[O] content was 10 ppm

lower in the steel balanced with slag A (a 68.75% decrease). The average oxygen content was lower than 15 ppm in all cases. There are many factors controlling the total oxygen in the steel (slag basicity, CaO/Al$_2$O$_3$ ratio, slag oxidizability, and content of deoxidizing elements, *etc.*), in addition to some other dynamics conditions. Except for the different components of the slag, the other conditions were basically the same in comparative experiments. Figures 9 and 10 show the relationship between the CaO/Al$_2$O$_3$ ratio and the integrated basicity of the slag and the T[O] content in the steel. The T[O] content showed a gradual decreasing trend with the (CaO+MgO)/SiO$_2$ and CaO/Al$_2$O$_3$ ratios (the average total oxygen content decreased from 22.17 to 9.56 ppm in the steel). With increasing CaO/Al$_2$O$_3$ ratio, free oxygen ions were released and subsequently bound to CaO and Al$_2$O$_3$. As a result, the optical basicity and the sulphur capacity of the slag increased significantly, thereby greatly favouring deoxidation and desulphurization from the point of view of thermodynamics.

Control of the steel inclusions with different slag systems under equilibrium conditions

The inclusions essentially comprised the Al$_2$O$_3$ system in blank steel samples and a minor fraction of the MnO–Al$_2$O$_3$–SiO$_2$ system after the metal–slag reaction. A total of 221 inclusions were observed in the steel samples balanced with slag A, and were divided into four types:

(1) Calcium magnesium aluminum silicate (69.7% of the total)
(2) Calcium manganese aluminum silicate (10.4%)
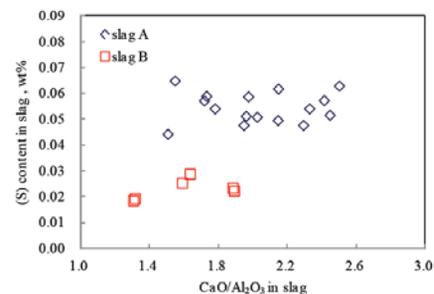(3) Magnesia alumina spinel (4.1%)
(4) Alumina (1.8%).

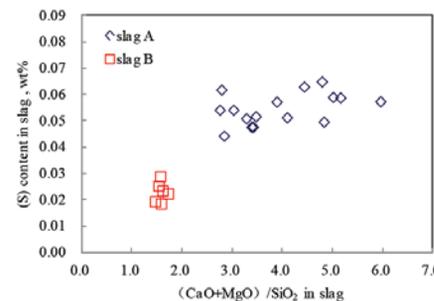Figure 7—S content as a function of the CaO/Al$_2$O$_3$ ratio in the slag

Figure 8—S content as a function of the (CaO+MgO)/SiO$_2$ ratio in the slag

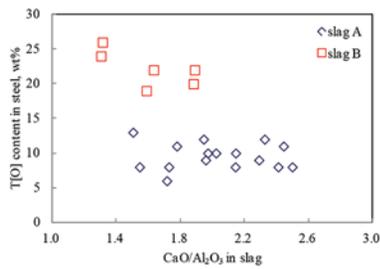# Effect of different refining slag systems on the cleanliness of molten steel

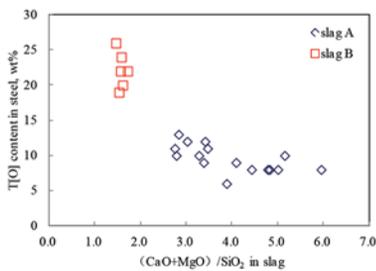Figure 9—T[O] content in the steel as a function of the CaO/Al_2O_3 ratio

Figure 10—T[O] content in the steel as a function of the $(CaO + MgO)/SiO_2$ ratio

The statistics, including the size distributions and types of main inclusions, are listed in Figure 11a.

A total of 127 inclusions were observed in steel samples under equilibrium conditions with slag B. Nonmetallic inclusions mainly existed as three types:

(1) Calcium manganese aluminum silicate (84.25% of the total
(2) Aluminosilicate (5.51%)
(3) Alumina (10.24%).

The statistics are shown in Figure 11b.

Most of the observed inclusions were spherical under the two slag systems, with a minor fraction being nearly spherical. These results can be explained as follows. The CaO content of the inclusions was not sufficiently high to modify the inclusions and they did not completely separate in the liquid phase at 1600°C. Most of the inclusions in the steel in balance with slag B (64.15% of the total) were less than 3 μm in size and comprised the $CaO–MnO–Al_2O_3–SiO_2$ system in liquid steel, while the inclusions of 3–5 μm in size accounted for 28.3%. Inclusions larger than 10 μm were not observed.

Most of the inclusions in the steel balanced with slag A were less than 3 μm in size and comprised the $CaO–MgO–Al_2O_3–SiO_2$ system. These inclusions accounted for 71.33% of the total number of inclusions, while those 3–5 μm in size accounted for 20.67% of the total. Only one inclusion larger than 10 μm was found. According to the above results and the types and distribution of inclusions in the test steel, the inclusions in the steel balanced with slag A were smaller than those in the steel balanced with slag B.

The $CaO–MgO–Al_2O_3–SiO_2$ nonmetallic inclusions mostly existed in liquid steel balanced with slag A. The chemical compositions of these inclusions were plotted on the $CaO–SiO_2–Al_2O_3$ ternary phase diagram. MgO and CaO inclusions can be considered together for this purpose. As can be seen from Figure 12, under the balance condition of slag system A, nearly half of the $CaO–MgO–Al_2O_3–SiO_2$ inclusions located within the area below the melting point of 1600°C in liquid carbon steel will form a liquid at the steelmaking temperature. The $CaO–MnO–Al_2O_3–SiO_2$ nonmetallic inclusions mostly existed in liquid steel balanced with slag B. Figure 13 show the chemical composition of these inclusions plotted on the $MnO–SiO_2–Al_2O_3$ ternary phase diagram. Under the balance condition of slag system B, a minor fraction of the $CaO–MnO–Al_2O_3–SiO_2$ inclusions showed melting points ranging from 1400 to 1600°C in liquid carbon steel. Numerous high-melting-point inclusions were located in the area of melting points greater than 1600°C, and the combined melting point should be higher than this value.
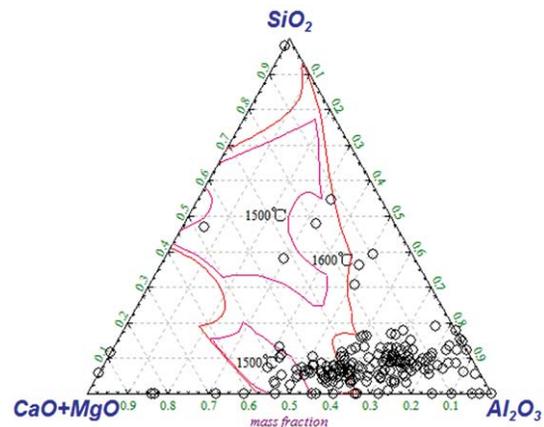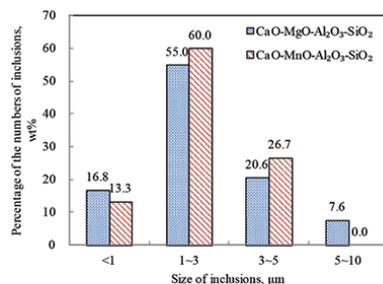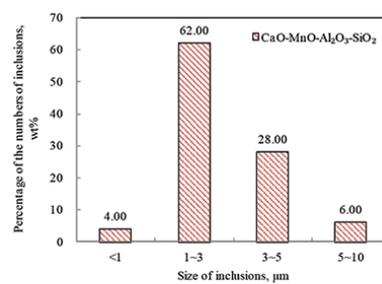

Figure 12—Compositions of inclusions in liquid steel balanced with slag A

(a) Slag A

(b) Slag B

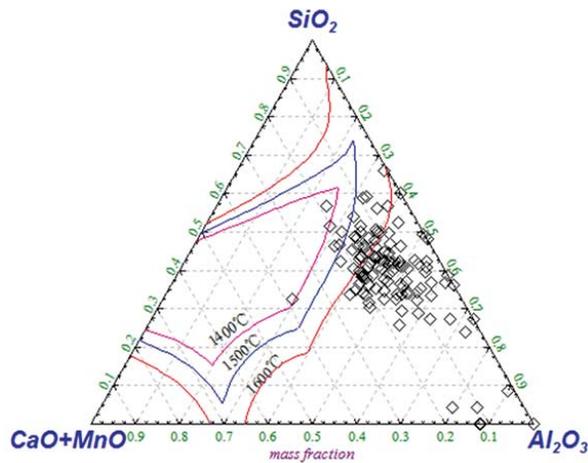Figure 11—Size distributions of main inclusions for both slags

Figure 13—Compositions of inclusions in liquid steel balanced with slag B

Factors influencing the inclusions components with different slag systems under equilibrium conditions

In order to improve the impact resistance of steel while avoiding anisotropy in the product, the inclusions should be low in number, small, and spherical. The melting point of the inclusions should be low so that they can be slightly modified to avoid hot tearing during the hot-rolling process. Additionally, the inclusions should be evenly distributed. Liquid $CaO–MgO–Al_2O_3–SiO_2$ and $CaO–MnO–Al_2O_3–SiO_2$ inclusions satisfy these requirements. As shown in Figures 12 and 13, a large number of inclusions were located in the liquid region with melting point lower than 1600°C. These two types of inclusions present in the steel sample were small and mostly spherical, as shown in Figures 14 and 15.

To generate liquid $CaO–MnO–Al_2O_3–SiO_2$ inclusions, slag system A (1.0–1.8 CaO/Al_2O_3 mass ratio and SiO_2 content 11–20 wt%) was reacted with liquid carbon steel. The thermodynamic calculations (details are not presented for reasons of brevity) showed that the inclusions were low-melting calcium aluminum silicate in the liquid carbon steel, when these equilibrium conditions are satisfied. The Al content was lower than 0.013 wt% in the equilibrium steel,

and the oxygen content was approximately 3 ppm. However, to generate liquid $CaO–MnO–Al_2O_3–SiO_2$ inclusions, slag system B (1.0–1.2 CaO/SiO_2 mass ratio and Al_2O_3 content of approximately 30 wt%) was used to balance with liquid carbon steel. In order to change the inclusions into low-melting aluminum silicate manganese in equilibrium liquid carbon steel, the following conditions need to be met. When the Al content is fixed at 0.0010–0.0015 wt% in molten steel, the oxygen activity is between 15 and 25 ppm under balance conditions. In summary, when slag system B reaches equilibrium with the liquid steel, the Al content in steel must be lower than that in the slag system A. In contrast to the slag system A, the oxygen content was relatively high and therefore the inclusions were mostly changed into $MnO–Al_2O_3–SiO_2$ inclusions in the steel in equilibrium with low-basicity slag B. These inclusions had higher melting points because the CaO content in the slag was lower, and the aluminum silicate manganese did not have enough time to transform into the low-melting-point $CaO–MnO–Al_2O_3–SiO_2$ inclusions. The $CaO–MgO–Al_2O_3–SiO_2$ inclusions were mostly low-melting-point inclusions in the liquid steel in equilibrium with the high-basicity slag A. The differences in the melting points of the inclusions can also be explained by the higher melting point of slag B compared to slag A. Thus, from a dynamics point of view, slag A is significantly superior to slag B.

Applications

Under the original process conditions, the castability of molten steel was poor, the opening position of the tundish stopper fluctuated continually, and the highest rising position was more than 15 mm. The stopper curve is shown in Figure 16a. In accordance with the XRD results for nodulation, nozzle clogging is mainly a result of the Al_2O_3 and $MgO–Al_2O_3$ inclusions. To overcome this issue and relieve the casting pressure, calcium wire was fed at the end of the refining process. After the refining slag improvement, the stopper opening and the mould level remained constant at a casting speed of 1.3 m/min, and the continuous casting process involved a total of 13 heats without Ca treatment. The stopper was only two times higher (≤ 5 mm) in the final
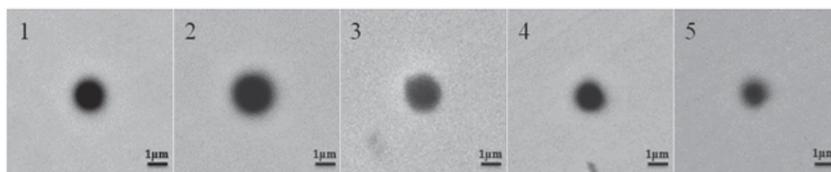

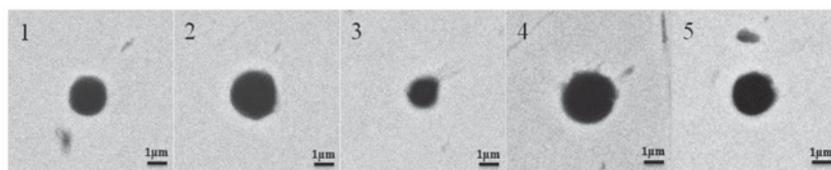**Figure 14—Morphology of typical $CaO–MgO–Al_2O_3–SiO_2$ inclusions**

Figure 15—Morphology of typical $CaO–MnO–Al_2O_3–SiO_2$ inclusions

(a) before optimization
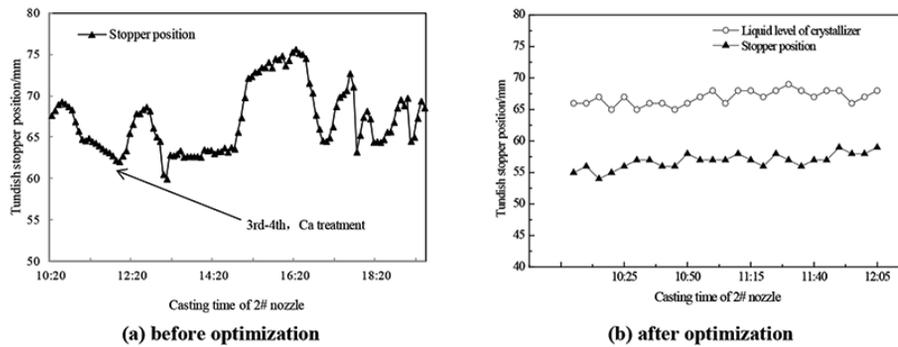

(b) after optimization

Figure 16—Tundish stopper curve (a) before and (b) after optimization

casting. The stopper curve is shown in Figure 16b. This indicates that the new refining process can improve the castability of carbon steel significantly.

Conclusions

➤ The T[O] content in the steel in equilibrium with slag A was between 6 and 13 ppm, which is 64% less than the original model. The majority (69.7%) of the total inclusions were CaO–MgO–Al$_2$O$_3$–SiO$_2$ inclusions. When the integrated basicity increased from 2.2 to 5.1 in the initial slag, the CaO/Al$_2$O$_3$ ratio increased from 1.0 to 1.8, and the T[O] and (FeO + MnO) contents decreased

➤ Under the equilibrium condition of slag B, the T[O] content of the steel was between 19 and 26 ppm, a decrease of 21% compared with the original model. CaO–MnO–Al$_2$O$_3$–SiO$_2$ inclusions accounted for 84.3% of the total number of observed inclusions. When the initial slag basicity increased from 1.0 to 1.2, the CaO/Al$_2$O$_3$ ratio increased from 0.8 to 1.5 while the T[O] content decreased

➤ When the CaO/Al$_2$O$_3$ ratio of the balanced slag increased to 1.3–1.9 (slag B) and to 1.5–2.5 (slag A), the slag basicity increased to 1.5–1.8 (slag B) and to 2.8–6.0 (slag A). Simultaneously, the average T[O] content in the steel decreased from 22.17 to 9.56 ppm, the average S content of the slag increased from 0.023 to 0.055 wt%, and the (FeO+MnO) content decreased from 0.82 to 0.50 wt%. The CaO/Al$_2$O$_3$ and (CaO+MgO)/SiO$_2$ ratios of slag A were higher, and the SiO$_2$ content and slag oxidability were lower than for slag B. Slag A therefore showed stronger deoxidizing and desulphurization abilities than slag B.

➤ The overall size of the CaO–MgO–Al$_2$O$_3$–SiO$_2$ inclusions in steel reacted with slag A was lower than that of the inclusions formed in the steel reacted with slag B. To generate spherical CaO–MgO–Al$_2$O$_3$–SiO$_2$ inclusions less than 3 μm in size while decreasing the T[O] and [S] contents in the steel, slag A is preferred as its CaO/Al$_2$O$_3$ ratio was between 1.2 to 1.8, and its SiO$_2$ content was in the range of 11–20 wt%.

Acknowledgement

References

Hu, G.C., Shen, J.G., and Zhang H, S.T. 2003. Carbon Structural Steel. China Standards Press, Beijing. 10 pp.

Huang, X.H. 2008. Principle for Iron and Steel Metallurgy. Metallurgy Industry Press, Beijing. 54 pp.

Jia, P.T., Hai, Y.F., and Song, W. 2001. Manual of Common Metal Materials in World. Jiangsu Science and Technology Press, Nanjing. 47 pp.

Li, L., He, S.P., and Zhang, G.X. 2010. Practice of reducing inclusion in Q235 slab for Chuanwei. *Iron Steel Vanadium Titanium*, vol. 31, no. 3. pp. 84–87.

Ohta, H. and Suito, H. 1996a. Activities in MnO-SiO$_2$-Al$_2$O$_3$ slags and deoxidation equilibria of Mn and Si. *Metallurgical and Materials Transactions B*, vol. 27B, no.4. pp. 263–270.

Ohta, H. and Suito, H. 1996b. Activities in CaO-SiO$_2$-Al$_2$O$_3$ slags and deoxidation equilibria of Si and Al. *Metallurgical and Materials Transactions B,* vol. 27B, no. 4. pp. 94–953.

Peng, Q.C., Li ,Y.Y., Yang, C.W., Chen, B.Q., Zou, W.J., Zhou, J., and Liu, G.M. 2007. Research on cleanliness of Q235B & SPHC steel grades produced by CSP technology. *Steelmaking*, vol. 23, no. 3. pp. 45–49.

Richard, H.R. and Chipman, J. 1965. Activities in the liquid solution SiO$_2$-CaO-MgO-Al$_2$O$_3$ at 1600°C. *Transactions of the Metallurgical Society of AIME*, vol. 233, no. 2. pp. 415–425.

Xu, Z.H., Yang, B., Li Q.J., and Lin, S.T. 2009. Control of nitrogen content in Q235 steel. *Hebei Metallurgy*, vol. 172, no. 4. pp. 26–27.

Yoon, B.H., Heo, K.H., and Kim, J.S. 2002. Improvement of steel cleanliness by controlling slag composition. *Ironmaking and Steelmaking,* vol. 29, no. 4. pp. 215.

Zhang, S.T., Wang, Z.L., and Xu, Q.A. 2003. Quality Carbon Structural Steel. China Standards Press, Beijing. 9 pp.

Zhi, J.G., Si, Y.T., Li, C.L., Liu, L., Yue, C.Q., and Tian, R.B. 2004. Cleanliness control of Q235B steel produced by CSP process for Baosteel. *Iron and Steel*, vol. 39 (suppl.). pp. 436–438. ◆